Charge transfer and transition-metal cluster: Boron bonding in the bct superconducting $Y(Rh_{1-x}Ru_x)_4B_4$ system

R. N. Shelton, H. E. Horng,* and A. J. Bevolo
Ames Laboratory—U.S. Department of Energy and Department of Physics, Iowa State University, Ames, Iowa 50011

J. W. Richardson and R. A. Jacobson
Ames Laboratory—U.S. Department of Energy and Department of Chemistry, Iowa State University, Ames, Iowa 50011

S. D. Bader and H. C. Hamaker
Materials Science and Technology Division, Argonne National Laboratory, Argonne, Illinois 60439
(Received 22 November 1982)

An analysis of the bonding and charge transfer as a function of transition-metal concentration is presented for the bct superconducting system $Y(Rh_{1-x}Ru_x)_4B_4$. A sharp drop in the superconducting critical temperature T_c from 9.5 K to below 1.0 K near a critical concentration is not reflected in the smooth, linear variation of the single-crystal lattice parameters and B-B interatomic distances. Analysis of the boron *KVV* Auger data indicates the boron *p*-like states near the Fermi energy are increasingly populated in a continuous manner with increasing x. We find no evidence of any abrupt changes in the electronic structure near x_{cr}.

I. INTRODUCTION

The unusual low-temperature superconducting and magnetic properties of $CeCo_4B_4$-type primitive tetragonal rare-earth ternary borides[1–10] RRh_4B_4 and Chevrel-phase compounds $M_xMo_6S_8$ or $M_xMo_6Se_8$ (Refs. 11 and 12) have attracted the attention of experimental and theoretical solid-state physicists. Since the discovery of these ternary phases, the interaction between superconductivity and long-range magnetic order has generated renewed interest from both theoretical[13,14] and experimental[15,16] standpoints. During the last five years, numerous new ternary boride phases involving rare-earth elements have been discovered, such as the body-centered tetragonal $LuRu_4B_4$,[8] hexagonal $CeCo_3B_2$,[17–21] and orthorhombic $LuRuB_2$.[22,23] One of the major reasons for the considerable interest in ternary borides is not only the complexity of boron chemistry which yields many ternary boride phases with extremely different low-temperature properties, but also the occurrence of superconductivity in the presence of an ordered sublattice of magnetic rare-earth ions. As the number and variety of known ternary superconducting phases increases, the need to discern any systematic behavior of the superconducting properties of these complex materials becomes more acute. Many of these boride-based phases offer the opportunity to study the fundamental physics of the interaction between superconductivity and magnetism. A great deal of recent research has been devoted to pseudoternary boride systems such as $(R^1_{1-x}R^2_x)Rh_4B_4$ (Refs. 24–30) and $R(Rh_{1-x}Ru_x)B_4$.[31,32] The rapidly increasing amount of available information on the crystallographic and physical properties of pseudoternary systems provides sufficient diversity and challenge to the researchers in this field. Previous reports on $Er(Rh_{1-x}Ru_x)_4B_4$ (Ref. 31) show that T_c remains essentially insensitive to Ru concentration over the range $0.05 \leq x \leq 0.40$. This plateau in T_c versus concentration is followed by an abrupt, drastic decrease in T_c over a very narrow critical concentration range. In order to investigate this phenomenon, samples in the isostructural system $Y(Rh_{1-x}Ru_x)_4B_4$ were synthesized and studied by single-crystal x-ray diffraction, Auger electron spectroscopy, and ac magnetic susceptibility measurements. The yttrium system was chosen to avoid possible complications due to a magnetic rare-earth element, as well as to prevent the superposition of rare-earth element and boron peaks in the Auger spectra. Single-crystal x-ray diffraction data and Auger spectra presented in this paper permit an analysis of the bonding and charge transfer over the whole transition-metal concentration range. Since

evidence for the existence of charge transfer and a relation between electronic distribution and the superconducting properties have already been presented for the Chevrel phase compounds,[33] an examination of such effects in the ternary borides provides further motivation for our experiments.

II. EXPERIMENTAL PROCEDURE

Two differently synthesized groups of samples were prepared for this study. In all cases, the melting steps were performed on a water-cooled copper hearth in a Zr-gettered argon arc furnace and mass losses were less than 0.1%. Group-1 samples were synthesized by a three-step process. Initially, the Rh:Ru ratio was fixed by arc melting the appropriate amounts of these two elements together into one ingot. Then the correct mass of boron was carefully melted into this ingot, followed by the final step of melting in a stoichiometric amount of Y. Auger spectra, single-crystal diffraction data, and ac susceptibility measurements were performed on these samples. Samples of group 2 were synthesized following these same three steps, but in addition were annealed in an argon atmosphere in a sealed tantalum tube according to the following schedule: 2.5 d at 1200 °C, 2 d at 1000 °C, and 3 d at 800 °C. This second group of samples was then powdered for χ_{ac} measurements to provide a check on the T_c versus composition dependence. Powder x-ray diffraction data for all samples in both groups indicated that the impurity phase content was less than the readily detectable limit of 5%.

Single crystals selected from group-1 ingots for accurate lattice constants and atomic positional parameters determination were roughly rectangular in shape with approximate dimensions of $0.3\times0.2\times0.2$ mm^3. The air-stable crystal was mounted on a glass fiber with epoxy and then placed on a computer-controlled four-circle automated dif-

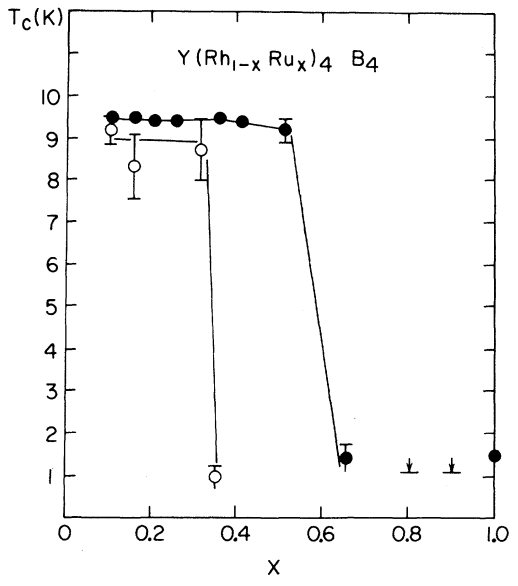

FIG. 1. Superconducting critical temperatures for group-1 (●) and group-2 (○) samples for the system $Y(Rh_{1-x}Ru_x)_4B_4$ plotted vs transition-metal concentration. Error bars on T_c indicate the width of the transition into the superconducting state. The symbol ⊥ indicates no superconducting state was found above 1.05 K and ⊤ indicates a transition into the superconducting state had begun, but was not completed.

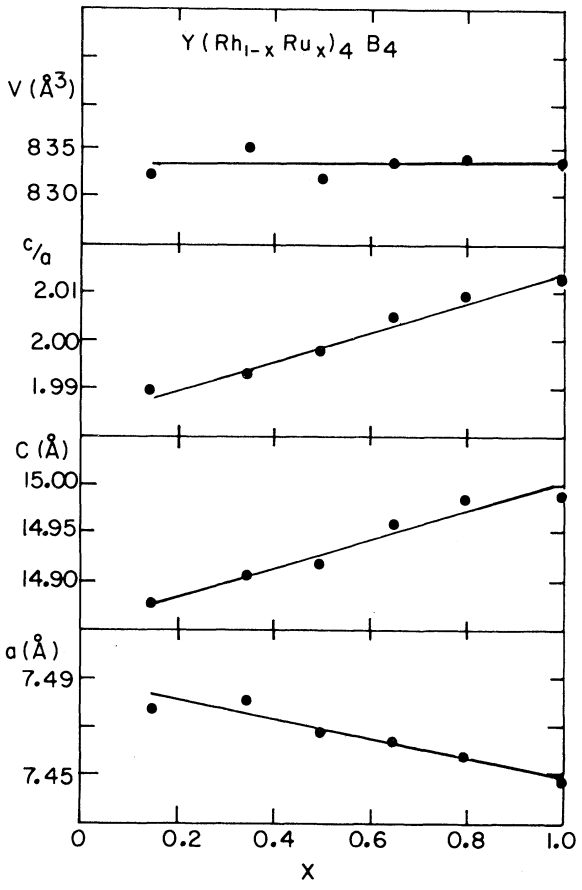

FIG. 2. Body-centered tetragonal lattice parameters, c/a ratio, and unit cell volumes for the system $Y(Rh_{1-x}Ru_x)_4B_4$ plotted vs transition-metal concentration. The size of the dots represents the uncertainty in determining the lattice parameters from single-crystal x-ray diffraction data.

fractometer.[34] Monochromated molybdenum $K\alpha$ radiation was applied throughout the data collection process (wavelength $\lambda=0.709\,54$ Å). The data were corrected for Lorentz and polarization effects. Inspection of a three-dimensional Patterson map led to initial placement of the metal atoms. Scattering factors used were those of Hanson *et al.*[35] with the metal-atom scattering factors corrected for real and imaginary effects due to anomalous dispersion.[36] For each of six compositions, the positional parameters and temperature factors were refined by least-squares techniques, yielding R values from 3.2% to 7.0%. Interatomic distances were calculated using the refined metal-atom positions and symmetries of the space group $I4_1/acd$ (no. 142).

In the Auger electron spectroscopy (AES) experiments, samples with polished surfaces about 0.1 cm thick, 0.2 cm wide, and 0.5 cm long were mounted in the Auger spectrometer, which consisted of a Physical Electronic Model 10-155 cylindrical mirror analyzer with a coaxial 5-keV electron gun. The analyzer had an energy resolution of 0.6%. The electron beam with 3-keV energy and 2.0-μA current had a spot size of approximately 100 μm. An intensive Ar^+-ion bombardment at 3 keV with a current density near 100 $\mu A/cm^2$ was required to clean the sample's surface and remove the influence of oxygen and carbon contamination on the boron line shape. Only the boron peaks, which were part of a more complete spectra covering the energy range from 50 to 300 eV, are reported in this paper.

III. RESULTS AND DISCUSSION

Ternary superconductors often include two metallic elements plus one nonmetal from column III*A*, IV*A*, V*A*, or VI*A* of the Periodic Table. The transition-metal clusters in superconducting compounds are often an important crystallographic feature related to the superconducting properties, whereas the nonmetallic element may play a role in stabilizing the structure. The detailed nature of the complex crystallography as related to the superconducting properties is not well understood. From this point of view, the high-T_c borides provide a good experimental opportunity to explore the role of each element in a ternary superconducting system.

There are two significant features in the phase diagram shown in Fig. 1, which is obtained by ac susceptibility measurements on samples in as-cast, ingot form (group 1). First, we observe a plateau in T_c versus composition over the Ru concentration range $0.1 \leq x \leq 0.45$, followed by a dramatic depression in T_c over a rather narrow range with $x_{cr} \simeq 0.55$. This value of x_{cr} is comparable to the $x_{cr} \simeq 0.5$ for the $Er(Rh_{1-x}Ru_x)_4B_4$ system[31] and consistent with the results reported by Johnston,[37] whose samples were also arc-melted ingots. For the samples with concentration higher than $x=0.65$, no superconductivity was detected down to $T=1.1$ K except for the $x=1.0$ sample with $T_c=1.42$ K. Since the magnetic rare-earth element Er was replaced by nonmagnetic Y, it is not surprising that superconductivity occurs at the Ru-rich side in the Y system rather than the magnetic order observed in the Er system.[31]

Superconducting transition temperatures of the annealed group-2 samples are also presented in Fig. 1. Powdered samples, as opposed to ingots, were used to determine T_c in these ac susceptibility measurements. The differences between the data from group 1 and 2 are apparent. Transition widths are broader and the resulting critical concentration $x_{cr} \approx 0.35$ is much lower than observed for the ingots. A possible explanation is that material with $T_c \sim 9$ K exists only for $x \lesssim 0.35$, and the high T_c of the ingots with $0.35 \lesssim x \lesssim 0.55$ is due to screening the bulk of the sample by a small amount of material with $x \lesssim 0.35$. We note that the smooth variation of lattice parameters shown in Fig. 2 for group-1 samples indicates the presence of a continuous bct phase for $0.15 \leq x \leq 1.0$, thus arguing against a limited phase region. A second explanation is that the pulverizing process could introduce strain into the lattice, resulting in the observed broadening of the transition into the superconducting state. In order to isolate possible effects on x_{cr} and T_c due to this pulverization from effects due to annealing, we also completed ac susceptibility measurements on group-1 samples in powdered form. Although the resulting transitions were broad ($\Delta T_c \sim 1.5$ K), the value of x_{cr} remained constant at 0.55, indicating that the strain introduced by the pulverizing process simply broadens the transition and is not the cause of the change in x_{cr}. We conclude that the shift in x_{cr} is due to the annealing process by affecting the degree of disorder and randomness within the transition-metal sublattice, which influences the superconducting properties of these compounds as discussed below.

Although T_c changes sharply with transition-metal concentration, the room-temperature single-crystal lattice parameters vary smoothly and linearly, consistent with Vegaard's law. Lattice parameters, c/a ratio, and unit cell volume are shown in Fig. 2. The linear behavior of these data is similar to that in the Er system[31]; however, the published lattice parameters obtained from powder x-ray diffraction for the Er system have a much greater un-

TABLE I. Structure data for $Y(Rh_{1-x}Ru_x)_4B_4$ compounds at room temperature. Standard deviations are in parentheses.

		Y			Rh-Ru			B		
Sample	x	y	z	x	y	z	x	y	z	R
$Y(Rh_{0.85}Ru_{0.15})_4B_4$	0	0.25	0.125	0.1169(2)	0.4000(2)	0.4383(1)	0.827(2)	0.107(2)	0.957(1)	0.045
	0	0.25	0.125	0.1167(2)	0.4009(2)	0.4384(1)	0.823(3)	0.112(2)	0.957(1)	0.049
$Y(Rh_{0.65}Ru_{0.35})_4B_4$	0	0.25	0.125	0.1157(1)	0.3995(1)	0.4381(1)	0.829(2)	0.103(2)	0.956(1)	0.042
$Y(Rh_{0.50}Ru_{0.50})_4B_4$	0	0.25	0.125	0.1147(1)	0.3990(1)	0.4375(1)	0.832(2)	0.104(2)	0.959(1)	0.039
$Y(Rh_{0.35}Ru_{0.65})_4B_4$	0	0.25	0.125	0.1145(2)	0.3984(2)	0.4372(1)	0.833(2)	0.105(2)	0.956(1)	0.057
	0	0.25	0.125	0.1143(1)	0.3985(1)	0.4371(1)	0.836(2)	0.107(1)	0.957(1)	0.032
$Y(Rh_{0.20}Ru_{0.80})_4B_4$	0	0.25	0.125	0.1145(2)	0.3983(2)	0.4369(1)	0.832(2)	0.104(2)	0.958(1)	0.055
	0	0.25	0.125	0.1145(2)	0.3983(2)	0.4369(1)	0.833(3)	0.105(2)	0.957(1)	0.057
YRu_4B_4	0	0.25	0.125	0.1154(2)	0.3983(2)	0.4369(1)	0.834(3)	0.105(2)	0.957(1)	0.070

certainty. It is interesting to note that $c/a=2$ at the critical concentration for these samples.

The structural data for $Y(Rh_{1-x}Ru_x)_4B_4$ compounds at room temperature are listed in Table I. For three single crystals, we collected two unique sets of diffraction data. Results from both sets are given in Table I and are indicative of the self-consistency of the methods. Low-temperature powder x-ray diffraction experiments done on four samples in this study ($x=0.15,0.35,0.65,1.0$) indicate no crystallographic transformation occurs from room temperature to 31 K.[38] Therefore, the systematic behavior of the room-temperature bct crystal structure parameters is also characteristic of the structure at low temperature where the superconducting properties are determined.

The crystal structure shown in Fig. 3 gives the atomic labeling which will be used in discussion of interatomic distances in these ternary compounds. In order to focus on the role of the transition-metal clusters, we label the ruthenium atoms 1 through 8 while roman numerals I, II, III are used for the bo-

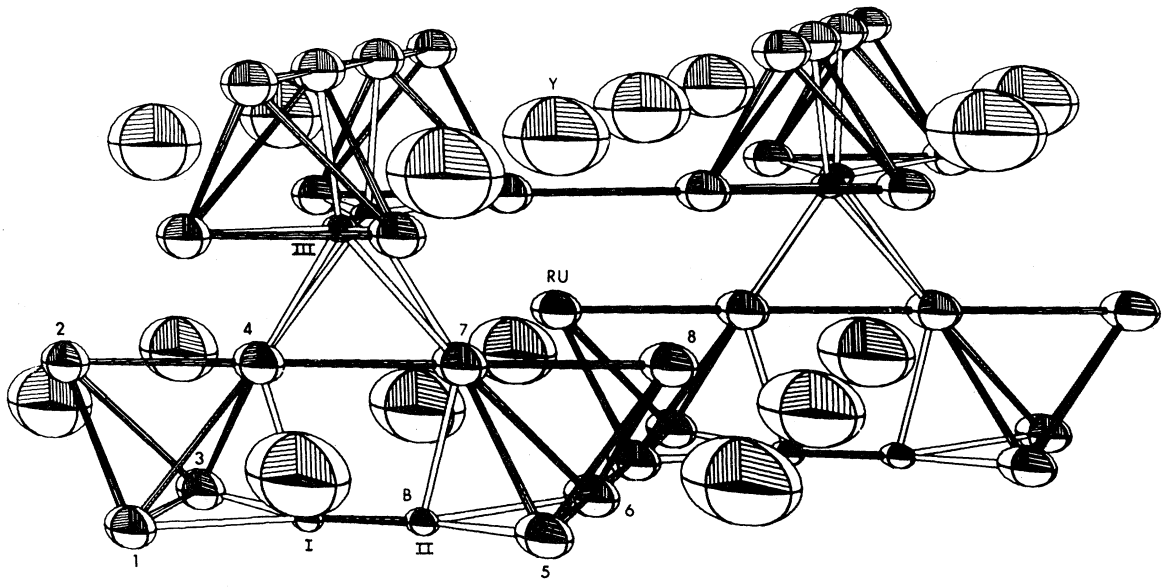

FIG. 3. One-half of the unit cell of YRu_4B_4. The x axis is directed up the page, the y axis across the page from left to right and the z axis into the page.

ron atoms. From single-crystal x-ray diffraction data, the intercluster and intracluster Ru-Ru distances display the very interesting results shown in Fig. 4. We observe that all Ru-Ru distances for Ru atoms within the same tetrahedral cluster (● and ■) decrease linearly with increasing x until a minimum at $x=0.80$ is reached. These intracluster distances then increase slightly with increasing x between $x=0.80$ and $x=1.00$. In contrast, the intercluster Ru-Ru distance (▲) between two clusters in the same zigzag chain increases linearly with increasing x, attaining a maximum at $x=0.80$. Upon further increasing x, this distance decreases. From this observation, it is apparent that the size of the Ru tetrahedral cluster and the degree of distortion are very sensitive to the concentration x. Comparing what we obtained from this figure with the T_c versus composition phase diagrams, one observes that as x increases from 0.15 to 0.80 the Ru tetrahedral cluster contracts, the intercluster distance increases, and the superconducting properties change from a high-T_c plateau to a region with no T_c above 1.1. K. As x increases from 0.80 to 1.0, the cluster expands, and the distance between two clusters decreases and superconductivity appears again at $x=1.0$.

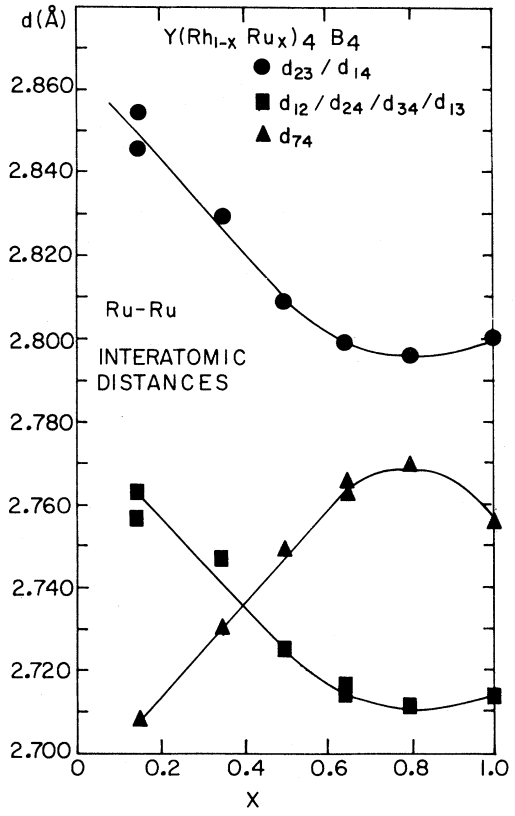

FIG. 4. Ru-Ru interatomic distances for the system $Y(Rh_{1-x}Ru_x)_4B_4$ plotted vs transition-metal concentration. Two data points for the same concentration represent the results from the same single crystal with different data collection.

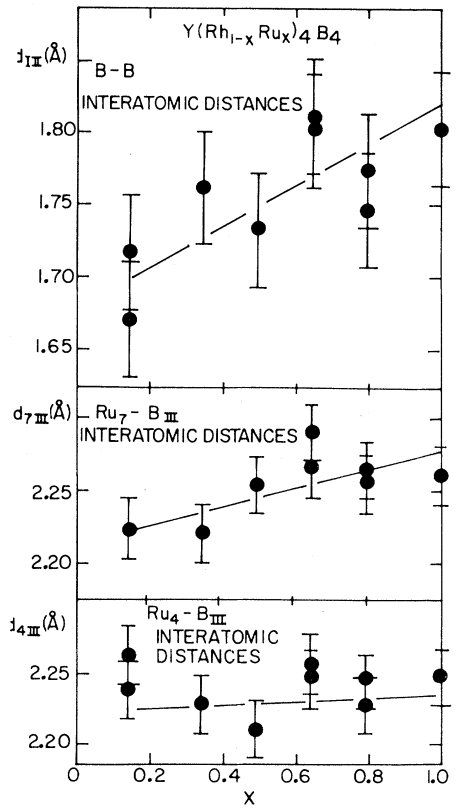

FIG. 5. B_I-B_{II}, Ru_7-B_{III}, and Ru_4-B_{III} interatomic distances for the system $Y(Rh_{1-x}Ru_x)_4B_4$ plotted vs transition-metal concentration. Error bars represent standard deviations.

The interatomic distances involving boron are shown in Figs. 5 and 6 and have relatively large error bars. This is due to the greater uncertainty in determining the boron position. Several efforts were made to improve the boron positional parameters; anisotropic temperature factors and analysis of curvatures in electron density difference maps were tried, but without any success. The major impediment is the small scattering factor of boron compared to the other elements in the structure. Taking this large uncertainty into account, the distance between boron pairs is a linearly increasing function of Ru concentration x. These results on samples with

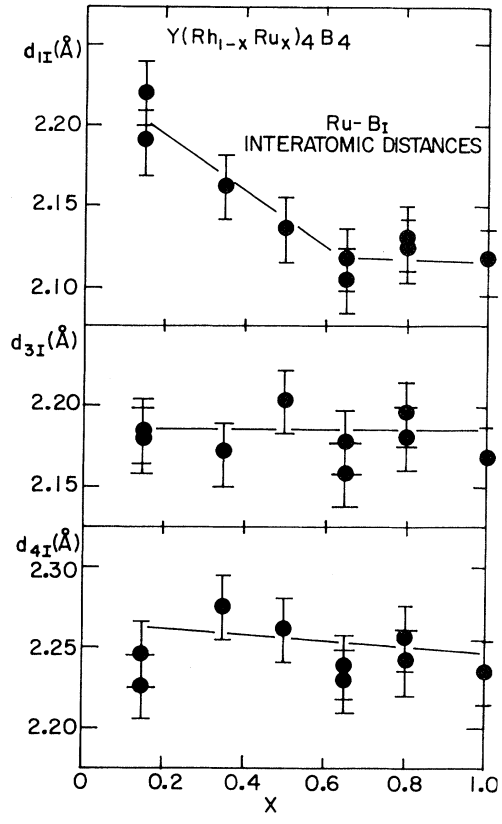

FIG. 6. Ru_1-B_I, Ru_3-B_I, and Ru_4-B_I interatomic distances for the system $Y(Rh_{1-x}Ru_x)_4B_4$ plotted vs transition-metal concentration. Error bars indicate standard deviations.

six different compositions in this paper are similar to the data on five samples published by Yvon and Grüttner[39] and analyzed by Johnston.[37] In fact, the overall consistency between the atomic positional parameters determined by Yvon and Grüttner[39] (their Table I) and those of the present study is evident by direct comparison (our Table I). However, close inspection of these earlier data[39] indicates that one composition with an anomalous boron positional parameters ($x=0.50$) is predominantly responsible for the sharp decrease of the B-B interatomic spacing at $x=0.50$. Examination of the nearly horizontal functions of the interchain distance Ru_7-B_{III} and Ru_4-B_{III} indicates that the substitution of Rh by Ru does not alter the interaction between the atoms in two different zigzag chains.

Shown in Fig. 7 are the derivative B *KVV* Auger spectra for a set of $Y(Rh_{1-x}Ru_x)_4B_4$ compounds which span the complete compositional range. It is immediately clear from the dominant spectral features that a continuous evolution of the line shape takes place on varying x. Thus our Auger results are not compatible with Johnston's[37] model, which predicts an *abrupt* change in the electronic structure at x_{cr}. Vertical guidelines in Fig. 7 delineate predominantly *ss*, *sp*, and *pp* regions of the spectra, as will be elucidated in the analysis below. The Rh-rich compounds differ markedly from the Ru-rich compounds, as indicated especially by the asymmetry in the important *pp* trough near E_F for the former compounds. Although the spectra have not been corrected for electron-energy-loss effects, it is shown elsewhere that the loss background that contributes to their low-energy regions are featureless and similar.[40] Furthermore, the possibility that the observed characteristics are influenced by overlap with the Rh $M_{45}N_1N_{23}$ line, which occurs in this energy range, was eliminated in a separate experiment by use of a primary beam energy near the Rh M_{45} threshold.[40] Therefore, the uncorrected data shown in Fig. 7 are good representations of the features of the B *KVV* lines.

The data shown in Fig. 8, which plots the Auger spectra for RuB, RhB, YRu_4B_4, and primitive tetragonal YRh_4B_4, suggest that the shape of the B *KVV* line is primarily determined by the M—B bonds (M=Rh,Ru). Comparison between the corresponding binary and ternary boride data reveals remarkably similar qualitative behaviors. Also, the YRh_4B_4 and $Y(Rh_{0.85}Ru_{0.15})_4B_4$ spectra are nearly identical in spite of their different crystal structures.

In order to interpret the Auger spectra displayed in Fig. 7, a theoretical analysis was performed based on the band-structure calculations of Jarlborg, Freeman, and Watson-Yang[41] (JFW-Y) for YRh_4B_4. Although their results are for the $CeCo_4B_4$-type structure rather than the bct lattice of the $Y(Rh_{1-x}Ru_x)_4B_4$ compounds, the similarity of the local boron environment in each of the crystal structures suggests that the JFW-Y calculations provide valuable insights into the origin of the experimentally observed Auger features. Also, as noted above, we may expect from the nearly identical Auger spectra for YRh_4B_4 and $Y(Rh_{0.85}Ru_{0.15})_4B_4$ that differences in the density of states (DOS) are not serious.

The results of our analysis are summarized in Fig. 9. In Fig. 9(a), the JFW-Y results are shown for the B local DOS, with the Fermi energy E_F empirically shifted 1 eV to simulate the $x=0.15$ data. The peaks labeled s_1 and s_2 correspond roughly to the atomic charge and bonding components "in the Mulliken sense" of the B *s* DOS, respectively, and p_1 and p_2 refer to *pd* hybrid components which overlap with the upper and lower parts of the transition-metal *d* band. In Fig. 9(b), the calculated *ss*, *sp*, and

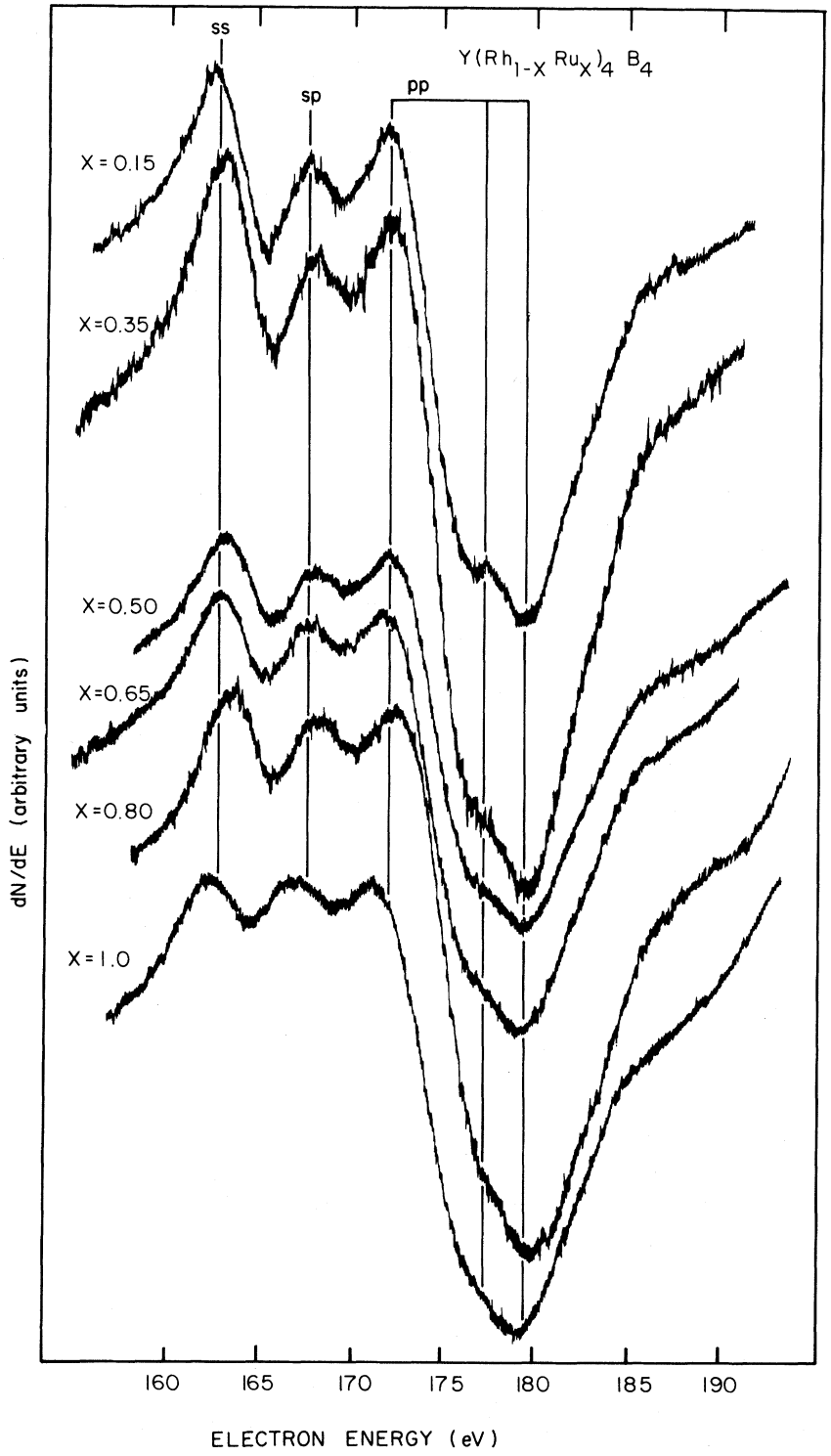

FIG. 7. Derivative B *KVV* Auger spectra for $Y(Rh_{1-x}Ru_x)_4B_4$. The vertical lines locate prominent features believed to be associated primarily with the indicated *ss*, *sp*, or *pp* folds of the B local DOS.

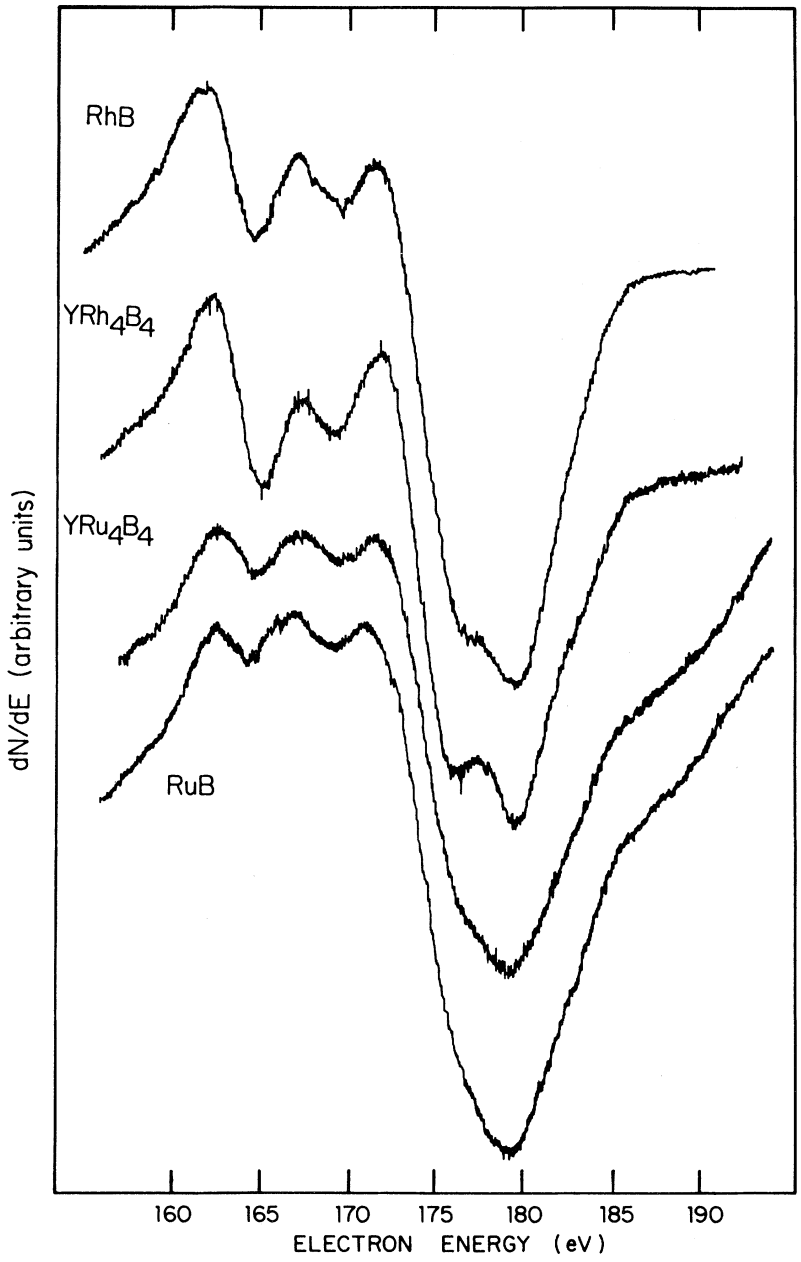

FIG. 8. Derivative B *KVV* Auger spectra for RhB, YRh_4B_4, YRu_4B_4, and RuB.

pp self-folds are shown (note the doubling of the energy axis), as well as their sum, broadened by $\Gamma=1$ eV halfwidth at half maximum (HWHM) to simulate predominantly analyzer-resolution and core-hole—lifetime effects. In this analysis, Auger matrix elements α_{ij} were set to unity, and the muffin-tin radius of the JFW-Y calculations determined the relative weighting of the $ij=ss$, sp, and pp terms. The derivative spectra are shown in Fig. 9(c) with and without the 1-eV shift of E_F, and the vertical guidelines reproduced from Fig. 7 indicate the good agreement with the Rh-rich and Ru-rich experiments, respectively, especially in the *pp* region. (The experimental guidelines were positioned with E_F at 185 eV $=E_K-\phi_a$, where E_K is the B 1*s*-subshell binding energy with respect to E_F, and ϕ_a is the analyzer work function.) Adjustments of the noncritical parameters α_{ij} and Γ could improve agreement in the problematic *sp* region, where the calculations show two shallow features instead of one.

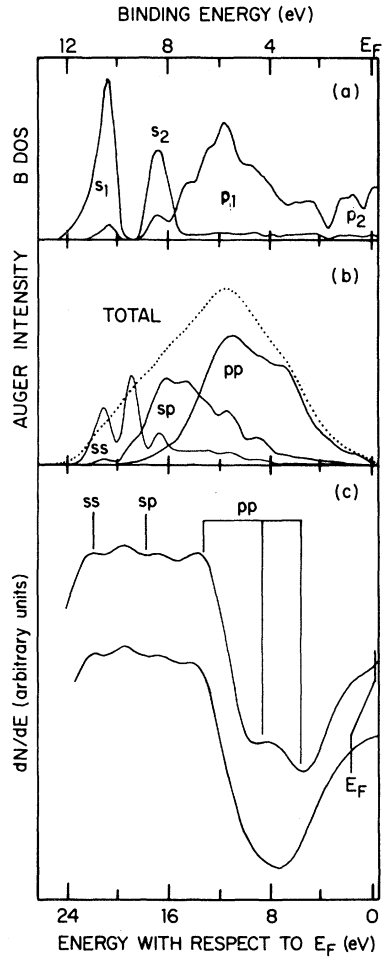

FIG. 9. Summary of the B *KVV* line-shape analysis. (a) B local DOS calculated by Jarlborg *et al.* (Ref. 41) with E_F shifted by 1 eV. (b) Calculated *ss*, *sp*, and *pp* folds of the B valence band. The curve labeled "total" is the Gaussian-broadened sum of the component folds. (c) Derivative of the "total" spectrum (upper curve) and that calculated without the 1-eV shift of E_F, as indicated (lower curve). The *ss*, *sp*, and *pp* guidelines are transferred from Fig. 7.

The above Auger analysis suggests that the B *p*-like states near E_F, denoted as p_2 in Fig. 9(a), are increasingly populated in a continuous manner as x increases. In particular, the Auger data show no evidence of any abrupt changes in the electronic structure near the critical concentration at which T_c sharply decreases. The current study does not support the model proposed by Johnston[37] which attributed the increase in T_c to an abrupt electron transfer from the B dimers, which had been acting as electron "sinks" for the extra Rh electron, to a high DOS peak at E_F associated with the transition-metal sites. Instead, the data suggest that occupation of the p_2 states modifies the nature of the B-*M pd*-electron hybridization. It has been noted previously[31,37] that changes in the c/a ratio with x correlate with the T_c variation; for c/a greater (less) than 2, the $R(Rh_{1-x}Ru_x)_4B_4$ compounds are low- (high-) T_c materials, and the M_4 tetrahedra are prolate (oblate). It is possible that the change of the *pd* hybridization with x may cause the observed distortion. Such distortions may produce anisotropies that enhance the electron-phonon interaction. Similar distortions of the M_4 tetrahedra have been observed in related pseudoternaries, such as $Er(Rh_{1-x}Ir_x)_4B_4$,[10] in the T_c switch-over region. A microscopic description of the relationship between such structural distortions and the strength of the electron-phonon coupling would be useful.

Alternatively, Ku *et al.*[42] have suggested that the sharp drop in T_c for $x > 0.5$ may result from less than half of the M_4 tetrahedra being composed entirely of Rh atoms, which are thought to be primarily responsible for the high values of T_c. Such a theory would require, of course, that the Rh and Ru (or Ir) atoms do not randomly occupy the M_4 tetrahedra, but instead segregate to maximize the number of "pure" Rh_4 and Ir_4 clusters. These ideas are consistent with both the Auger spectra and the observed shift with annealing of the concentration at which T_c drops. As Ku and co-workers have suggested,[42] diffuse x-ray scattering could confirm the existence of such segregation. Conversely, high-pressure studies performed on single crystals under uniaxial stress might more clearly reveal the effects of structural distortions upon T_c.

ACKNOWLEDGMENTS

Ames Laboratory is operated for the U. S. Department of Energy by Iowa State University under Contract No. W-7405-Eng-82. The research at Ames Laboratory was supported by the Director for Energy Research, Office of Basic Energy Sciences, WPAS-KC-02-02-02 and WPAS-KC-02-03-01. Argonne National Laboratory is also supported by the U. S. Department of Energy.

*Permanent address: Department of Physics, National Taiwan Normal University, Taipei, Taiwan, Republic of China.

[1]B. T. Matthias, E. Corenzwit, J. M. Vandenberg, and H. E. Barz, Proc. Natl. Acad. Sci. U. S. A. 74, 1334 (1977).

[2]J. M. Vandenberg and B. T. Matthias, Proc. Natl. Acad. Sci. U. S. A. 74, 1336 (1977).
[3]Yu. B. Kuz'ma and N. S. Bilonizhko, Kristallografiya 16, 1030 (1971) [Sov. Phys.—Crystallogr. 16, 897 (1972)].
[4]A. Grüttner and K. Yvon, Acta. Crystallogr. Sect. B 35, 451 (1979).
[5]P. Rogl, Monatsh. Chem. 110, 235 (1979).
[6]P. Rogl, Monatsh. Chem. 111, 517 (1980).
[7]Yu. B. Kuz'ma and N. S. Bilonizhko, Dopov. Akad. Nauk Ukr. RSR Ser. A 3, 275 (1978).
[8]D. C. Johnston, Solid State Commun. 24, 699 (1977).
[9]H. C. Ku, D. C. Johnston, B. T. Matthias, H. Barz, G. Burri, and L. Rinderer, Mater. Res. Bull. 14, 1591 (1979).
[10]H. C. Ku, B. T. Matthias, and H. Barz, Solid State Commun. 32, 937 (1979).
[11]Ø. Fischer, A. Treyvaud, R. Chevrel, and M. Sergent, Solid State Commun. 17, 21 (1975).
[12]R. N. Shelton, R. W. McCallum, and H. Adrian, Phys. Lett. 56A, 213 (1976).
[13]E. I. Blount and C. M. Varma, Phys. Rev. Lett. 42, 1079 (1979).
[14]C. G. Kuper, M. Revzen, and A. Ron, Phys. Rev. Lett. 44, 1545 (1980).
[15]*Ternary Superconductors,* edited by G. K. Shenoy, B. D. Dunlap, and F. Y. Fradin (North-Holland, New York, 1981).
[16]W. A. Fertig, D. C. Johnston, L. E. DeLong, R. W. McCallum, M. B. Maple, and B. T. Matthias, Phys. Rev. Lett. 38, 987 (1977).
[17]Yu. B. Kuz'ma, P. I. Kripyakevich, and N. S. Bilonizhko, Dopov. Akad. Nauk Ukr. RSR Ser. A 10, 939 (1969).
[18]K. Nühara and S. Yashima, Bull. Chem. Soc. Jpn. 46, 770 (1973).
[19]P. Rogl, Monatsh. Chem. 106, 1624 (1975).
[20]I. P. Valovka and Yu. B. Kuz'ma, Inorg. Mater. 14, 356 (1978).
[21]H. C. Ku, G. P. Meisner, F. Acker, and D. C. Johnston, Solid State Commun. 35, 91 (1980).
[22]R. N. Shelton and H. C. Ku, Mater. Res. Bull. 15, 1445 (1980).
[23]H. C. Ku and R. N. Shelton, Mater. Res. Bull. 15, 1441 (1980).
[24]D. C. Johnston, W. A. Fertig, M. B. Maple, and B. T. Matthias, Solid State Commun. 26, 141 (1978).
[25]R. N. Shelton, C. U. Segre, and D. C. Johnston, Solid State Commun. 33, 843 (1980).
[26]M. Ishikawa, Phys. Lett. 74A, 263 (1979).
[27]K. Okuda, Y. Nakakura, and Kadowaki, Solid State Commun. 32, 185 (1979).
[28]C. Y. Huang, S. E. Kohn, S. Kaekawa, and J. L. Smith, Solid State Commun. 32, 929 (1979).
[29]S. Maekawa, J. L. Smith, and C. Y. Huang, Phys. Rev. B 22, 164 (1980).
[30]H. Adrian, K. Muller, and G. Saemann-Ischenko, Phys. Rev. B 22, 4424 (1980).
[31]H. E. Horng and R. N. Shelton, in *Ternary Superconductors,* edited by G. K. Shenoy, B. D. Dunlap, and F. Y. Fradin (North-Holland, New York, 1981), p. 213.
[32]Y. Muto, H. Iwasaki, T. Susaki, N. Kobayashi, M. Ikebe, and M. Isino, in *Ternary Superconductors,* edited by G. K. Shenoy, B. D. Dunlap, and F. Y. Fradin (North-Holland, New York, 1981), p. 197.
[33]K. Yvon and A. Paoli, Solid State Commun. 24, 41 (1977).
[34]W. J. Rohrbaugh and R. A. Jacobson, Inorg. Chem. 13, 2535 (1974).
[35]H. P. Hanson, F. Herman, J. D. Lea, and S. Skillman, Acta Crystallogr. 17, 1040 (1960).
[36]D. H. Templeton, in *International Tables for X-Ray Crystallography,* edited by C. H. MacGillavry, G. D. Rieck, and K. Lonsdale (Kynoch, Birmingham, England, 1962), Vol. III, pp. 215, Table 3.3.2c.
[37]D. C. Johnston, Solid State Commun. 42, 453 (1982).
[38]H. E. Horng, Ph.D. thesis, Iowa State University, 1982 (unpublished).
[39]K. Yvon and A. Grüttner, in *Superconductivity in d- and f-Band Metals,* edited by H. Suhl and M. B. Maple (Academic, New York, 1980), p. 515.
[40]H. C. Hamaker, G. Zajac, and S. D. Bader, following paper, Phys. Rev. B 27, 6713 (1983).
[41]T. Jarlborg, A. J. Freeman, and T. J. Watson-Yang, Phys. Rev. Lett. 39, 1032 (1977).
[42]H. C. Ku, F. Acker, and B. T. Matthias, Phys. Lett. 76A, 399 (1980).